International Journal of Engineering Research & Technology (IJERT)
ISSN: 2278-0181
Vol. 11 Issue 11, November-2022

Modeling and Controller Design of a Bidirectional DC-DC Converter for Electric Vehicles System

Solomon Habtamu (M.Sc.), [1] Kifle Godana (M.Sc.), [2]

1. Faculty of Electrical and Computer Engineering, Jimma University, Jimma Institute of Technology, Jimma, Ethiopia.
2. Faculty of Electrical and Computer Engineering, Jimma University, Jimma Institute of Technology, Jimma, Ethiopia.

***Abstract*:- Batteries are the primary energy-storage devices in application of electric vehicles. Battery fed electric drives are commonly being used for electric vehicles applications, due to various advantages, such as: approximately zero emission, definite load leveling, best transient operation and energy recovery during braking operation. To fulfill these requirements converters with bidirectional power flow capabilities are required to connect the accumulator (battery) to the dc link of the motor drive system. Battery fed electric vehicles is required to function in three different modes namely: acceleration mode, normal and braking mode. During acceleration and normal modes, the power flow is from battery to motor whereas during braking or regenerative mode the kinetic energy of the motor is converted into electrical energy and fed back to battery. The DC-DC converter is required to perform mainly two functions: first to match the battery voltage to the motor rated voltage and second to control the power flow under steady-state and transient conditions, so that the drive performance is as per the requirement. The proposed controller is adaptive PI controller for bi-directional dc-dc converter feeding a dc motor and its energy recovery due to regenerative braking has been demonstrated. The simulation and performance analysis of battery-operated electric vehicle under different drive condition are also presented through MATLAB/Simulink.**

Key words: Adaptive PI controller, Battery, Bidirectional DC-DC converter and Electric vehicles.

1. INTRODUCTION

In automobile industry, the general concept of electric vehicle refers to an electric drive vehicle using a battery or generator to convert from electric energy to mechanical energy. Now a day's bi-directional dc-dc converters are mostly used for several applications like as battery charger, electric vehicles and UPS systems. In case of the battery based electric vehicles, electric energy flows between motor and battery side [1]. For achieving zero emission, the vehicle can be powered only by batteries or other electrical energy sources. Batteries are adopted in ground vehicles because of their main features of high energy density, compact size, and reliability etc. That can be applied in electric vehicle with a battery as an energy storage element to provide desired management of the power flows [2,3]. Bidirectional DC-DC converters serves the purpose of stepping up or stepping down the voltage level between its input and output along with the capability of power flow in both the directions. This converter was used for the motor drives for the speed control and regenerative braking. It is employed when the DC bus voltage regulation has to be achieved along with the power flow capability in both the direction [4]. The converter topologies have been developed with soft switching technique to increase the transfer efficiency, zero-voltage switched (ZVS) technique and zero-current-switched (ZCS) technique were introduced for Bi-directional converter. Moreover, Bidirectional DC-DC converter exhibits challenging control problems, since it possesses highly non-linear characteristics and it involves frequent mode variation. Therefore, this study proposes a new approach for the bidirectional DC-DC converter adaptive controller.

2. MATHEMATICAL MODELING OF DC-DC CONVERTER

The mathematical modeling of half bridge non isolated bidirectional DC-DC converter is the combination of buck and boost converters. A non-isolated bi-directional dc-dc converter technology is to combine a buck and a boost converter in a half-bridge configuration. When charging the battery, this converter working as a buck converter, it operates in voltage step-down mode during the battery discharging its working as a boost converter; it operates in voltage step-up mode. The bidirectional dc-dc converter is placed in between high-voltage and low-voltage sources to allow energy transfer [5]. This kind of power converters use in many applications like in hybrid vehicles, in aerospace etc. Here a proposed modelling method is used based on modelling of each component individually, and then combining them to a complete model. The power stage was modelled using state-space averaging. After that the controllers are designed. The combined small-signal model generates all the transfer functions required for design purposes [6,7].

International Journal of Engineering Research & Technology (IJERT)
ISSN: 2278-0181
Vol. 11 Issue 11, November-2022

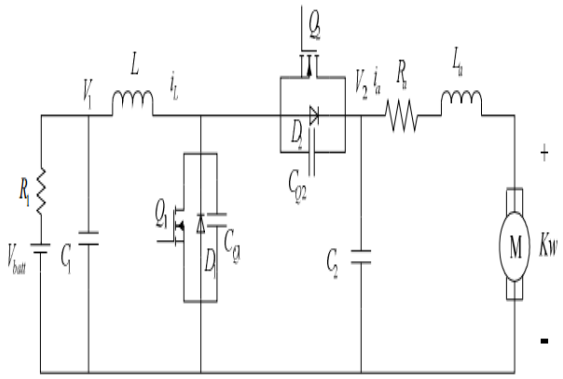

Fig.1 Block diagram of proposed Bidirectional DC-DC converter with PMDC.

Half bridge non-isolated bidirectional dc-dc converter fed PMDC motor is as shown in the Fig 1. It is operated in boost mode for forward motoring and in buck mode during electrical regeneration. Towards low-voltage side a battery pack is placed and on the other side a PMDC motor whose speed has to be controlled is installed [8,9]. It also contains a high-frequency capacitor as the energy buffer along the motor side as well as a smoothening capacitor along the battery side. Bidirectional dc-dc converter operating in the continuous conduction mode (CCM) requires a larger valued filter inductor. Thus, the inductor size increases and it also slows down the transient response and the mode transitioning. With the circuit operating in the discontinuous conduction mode (DCM), the inductor value can be considerably reduced and the response becomes faster, therefore power density increases. DCM operation also facilitates zero-turn on loss and thus low reverse recovery loss in diode. But at the same time the main switch is switched off at double the value of the average load current (i.e. at point d in Fig 3), therefore the losses during turn off increases. This can be reduced by using a snubber capacitor across the switches. Along with this, the inductor current also exhibits parasitic ringing during turning off of the switch as shown in Fig 2. This is because the switch's output capacitance in association with the inductor tends to oscillate and hence causes power dissipation and electrical stresses on the devices [7].

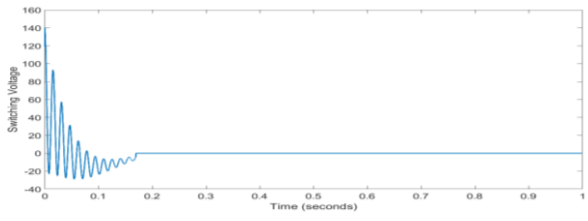

Fig 2. Parasitic Ringing of the Inductor Current

This is the major disadvantage associated with the DCM operation. The efficiency reduces because of all this Since it is desired that the converter should operate in the DCM, therefore the value of the inductor should be selected so as ensure DCM operation in both the modes. So as to ensure DCM operation of the converter for all the power negative effects of the DCM operation. Therefore, the soft switching techniques as well as the remedial measures for the parasitic ringing have to be ensured in the converter design.

This can be done by the incorporation of the complimentary gate switching technique as shown in the Fig 3[6].

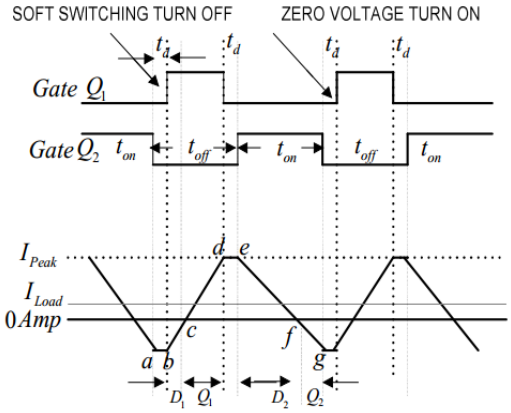

Fig 3. ZVRT soft switching technique [6].

Assume that the converter is operating in the boost motoring mode with the constant speed and fixed load torque so that the armature voltage and the inductor current are at steady state. Let initially the main switch Q1 is conducting as shown in the Fig 3. and hence the inductor current rises (c-d) till it reaches the dead (de) time when all the devices get turned off, and therefore the inductor current will charge the capacitor C Q1. Also, CQ2 will discharge to CQ1. Due to the presence of the snubber capacitors CQ1and CQ2the charging and discharging rates are reduced. Since the voltage across the capacitor cannot change abruptly, therefore the switching on and switching off losses are reduced. After this the inductor current flows through the diode D2 (e-f) and it decreases since voltage across capacitor C2 opposes it and finally it becomes zero at point f. After this it reverses its polarity through Q2 (f-g), thus the switch Q2 gets on at zero voltage because of the freewheeling current through D2. Also, the diode gets switched off at the zero voltage (at f) and therefore the reverse recovery losses are reduced. Again, the negative inductor current goes though switch Q2 which helps in charging CQ2 and discharging CQ1during the dead time and after that again the negative current is bypassed through diode D1 till it becomes zero and the switch Q1 turns on. Thus, the switch Q1 turns on at Zero Voltage condition. Here although the inductor current reaches zero value before the starting of the next cycle as in the normal DCM operation, but then also it is continuous because of the complimentary gate switching and the bidirectional conducting switches.

2.1 Modeling parameters of Converter

range, we can optimize the inductor value. It is necessary to optimize the inductance with all the design considerations. The relationship between inductor peak current *I*peak, minimum current *I*min, and inductor RMS current *I*RMS can

International Journal of Engineering Research & Technology (IJERT)
ISSN: 2278-0181
Vol. 11 Issue 11, November-2022

be expressed in (1.1) to (1.5), where *T*s is the switching period, *I*load is load current, *P* is the load power and Δ*I* is the inductor current ripple.

$$\Delta I = \frac{1}{2}\frac{v_{in} - v_o}{L}\frac{v_o}{v_{in}}T_s \qquad (1.1)$$

The optimization of the inductor design should satisfy the following conditions.

$$I_{peak} = I_{load} + \Delta I \qquad (1.2)$$

$$I_{load} = \frac{p}{v_o} \qquad (1.3)$$

$$I_{\min} = I_{load} - \Delta I \qquad (1.4)$$

$$I_{rms} = \sqrt{I_{load}^{\ 2} + \frac{\Delta I^2}{3}} \qquad (1.5)$$

2.1.1 Realization of ZVRT Soft Switching

From the above-described operation, it is found that the realization of gate signal
complementary control ZVRT soft switching depends on the emergence of inductor negative current, which can be acquired by limiting inductance to be less than the value *Lcr* expressed in (1.6). This inductance allows the converter operating under the boundary condition between DCM and CCM.

$$L_{cr} = \frac{1}{2}\frac{v_{in} - v_o}{p}\frac{v_o^{\ 2}}{v_{in}}T_s \qquad (1.6)$$

The capacitor values can be found out from the voltage ripple specification as given below:

$$C_1 = \frac{\Delta I}{8\Delta V_{IN}}T_s, C_2 = \frac{V_2 D}{R_A \Delta V_2}T_s \qquad (1.7)$$

3. Small-signal modeling of Bidirectional DC-DC converter State-space modeling

The mathematical models for the non-isolated bidirectional dc-dc converter have been developed for both the step-down and step-up mode operation in the continuous current conduction mode. State-space formulation method is employed for the modelling of the bi-directional dc-dc converter with the following assumptions [11]. It consists two operating modes, either battery charging mode or discharging mode, there are always two subintervals t_{on} and t_{off}. In the first subinterval, when the switch Q1 is on, and Q2 is off, the converter equivalent circuit can be represented in Fig 4(a).

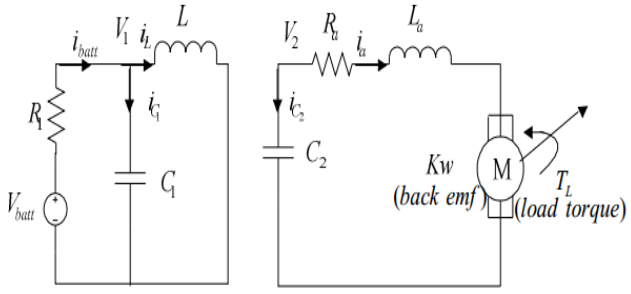

Fig 4(a) Equivalent circuit with Q1-on, Q2-off.

$$\begin{aligned}
\frac{di_L}{dt} &= \frac{V_1}{L} \\
\frac{di_a}{dt} &= -\frac{R_a}{L_a}i_a + \frac{V_2}{L_a} - \frac{K}{L_a}w \\
\frac{dV_1}{dt} &= \frac{V_{batt}}{R_1 C_1} - \frac{i_L}{C_1} - \frac{V_1}{R_1 C_1} \\
\frac{dV_2}{dt} &= -\frac{i_a}{C_2} \\
\frac{dw}{dt} &= \frac{K}{J}i_a - \frac{B_m}{J}w - \frac{T_L}{J}
\end{aligned} \qquad (1.8)$$

The state space representation of first subinterval is given as:

$$\begin{aligned}
\dot{X} &= A_1 X + B_1 U \\
Y &= C_1 X + D_1 U
\end{aligned} \qquad (1.9)$$

where $X = [i_l i_a V_1 V_2 w]^T, U = [V_{batt} T_L]^T, Y = [w]$

International Journal of Engineering Research & Technology (IJERT)
ISSN: 2278-0181
Vol. 11 Issue 11, November-2022

$$A_1 = \begin{bmatrix} 0 & 0 & \frac{1}{L} & 0 & 0 \\ 0 & -\frac{R_a}{L_a} & 0 & \frac{1}{L_a} & -\frac{K}{L_a} \\ -\frac{1}{C_1} & 0 & -\frac{1}{R_1 C_1} & 0 & 0 \\ 0 & -\frac{1}{C_2} & 0 & 0 & 0 \\ 0 & \frac{K}{J} & 0 & 0 & -\frac{B_m}{J} \end{bmatrix}$$

$$B_1 = \begin{bmatrix} 0 & 0 \\ 0 & 0 \\ \frac{1}{R_1 C_1} & 0 \\ 0 & 0 \\ 0 & -\frac{1}{J} \end{bmatrix}$$

$$C_1 = [0 \quad 0 \quad 0 \quad 0 \quad 1]$$

$$D_1 = [0]$$

(1.10)

In the second subinterval, when the switch Q1 is off, and Q2 is on, the converter equivalent circuit can be represented in Fig 4(b).

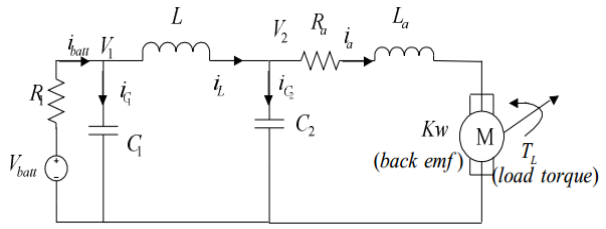

Fig 4(b): Equivalent circuit with Q1-off, Q2-on.

Similarly, circuit equations during second sub interval is given by

$$\frac{di_L}{dt} = \frac{V_1 - V_2}{L}$$

$$\frac{di_a}{dt} = -\frac{R_a}{L_a} i_a + \frac{V_2}{L_a} - \frac{K}{L_a} w$$

$$\frac{dV_1}{dt} = \frac{V_{batt}}{R_1 C_1} - \frac{i_L}{C_1} - \frac{V_1}{R_1 C_1} \qquad (1.11)$$

$$\frac{dV_2}{dt} = \frac{i_L}{C_2} - \frac{i_a}{C_2}$$

$$\frac{dw}{dt} = \frac{K}{J} i_a - \frac{B_m}{J} w - \frac{T_L}{J}$$

The state space representation is as follow for second subinterval

$$\dot{X} = A_2 X + B_2 U$$

$$Y = C_2 X + D_2 U \qquad (1.12)$$

Where

International Journal of Engineering Research & Technology (IJERT)
ISSN: 2278-0181
Vol. 11 Issue 11, November-2022

$$A_1=\begin{bmatrix} 0 & 0 & \frac{1}{L} & -\frac{1}{L} & 0 \\ 0 & -\frac{R_a}{L_a} & 0 & \frac{1}{L_a} & -\frac{K}{L_a} \\ -\frac{1}{C_1} & 0 & -\frac{1}{R_1C_1} & 0 & 0 \\ \frac{1}{C_2} & -\frac{1}{C_2} & 0 & 0 & 0 \\ 0 & \frac{K}{J} & 0 & 0 & -\frac{B_m}{J} \end{bmatrix}$$

$$B_1=\begin{bmatrix} 0 & 0 \\ 0 & 0 \\ \frac{1}{R_1C_1} & 0 \\ 0 & 0 \\ 0 & -\frac{1}{J} \end{bmatrix}$$

$$C_1=\begin{bmatrix} 0 & 0 & 0 & 0 & 1 \end{bmatrix}$$

$$D_1=\begin{bmatrix} 0 \end{bmatrix}$$

(1.13)

The state space average model of small signal system. Signal ac analysis for the different modes of the bidirectional converter operation under current mode control and also derives the transfer functions which describing the converter characteristics. The state variables of the above system are the capacitor voltages and the inductor current. Therefore, by considering ideal switching, the following two sets of state -space equations can be derived for each circuit state:

When Q1 is on the duty cycle is d(t):

$$\dot{X}=A_1x(t)+B_1u(t)$$
$$Y=C_1x(t)+D_1u(t) \qquad (1.14)$$

When Q2 is on the duty cycle is(1-d(t)):

$$\dot{X}=A_2x(t)+B_2u(t)$$
$$Y=C_2x(t)+D_2u(t) \qquad (1.15)$$

Where 't' is switching period. During each interval, since all the circuit parameters are constant equivalent circuit of the converter act like a time invariant system. But during switching between two modes the converter behaves like a time variant system. Then d(t)=(D+ d) Now assuming that operating point at equilibrium point and variation along operating point.

$$\frac{d}{dt}(X+x)=[A_1d(t)+$$
$$A_2(1-d(t))](X+x)+ \qquad (1.16)$$
$$[B_1d(t)+B_2(1-d(t))](U+u)$$

This equation indicates that the system is nonlinear which contains d , x and u . Valid assumption steady state is larger than small signal part therefore.

$$x.d\approx 0$$
$$ud\approx 0 \qquad (1.17)$$
$$\frac{dx}{dt}\approx 0$$

Now in linear approximation of the state space equations representing the averaged state space model.

International Journal of Engineering Research & Technology (IJERT)
ISSN: 2278-0181
Vol. 11 Issue 11, November-2022

$$\frac{dx}{dt} = Ax + Bu + [(A_1 - A_2)x + (B_1 - B_2)u]d$$

$$y = Cx + Du$$

(1.18)

Where

$$A = A_1 D + A_2(1-D)$$
$$B = B_1 D + B_2(1-D)$$
$$C = C_1 D + C_2(1-D)$$
$$D = D_1 D + D_2(1-D)$$

$$A = \begin{bmatrix} 0 & 0 & \frac{1}{L} & -\frac{1-D}{L} & 0 \\ 0 & -\frac{R_a}{L_a} & 0 & \frac{1}{L_a} & -\frac{K}{L_a} \\ -\frac{1}{C_1} & 0 & -\frac{1}{R_1 C_1} & 0 & 0 \\ \frac{1-D}{C_2} & -\frac{1}{C_2} & 0 & 0 & 0 \\ 0 & \frac{K}{J} & 0 & 0 & -\frac{B_m}{J} \end{bmatrix}$$

$$B = \begin{bmatrix} \frac{(1-D)V_2}{L} & 0 & 0 \\ 0 & 0 & 0 \\ 0 & \frac{1}{R_1 C_1} & 0 \\ -\frac{(1-D)i_L}{C_2} & 0 & 0 \\ 0 & 0 & -\frac{1}{J} \end{bmatrix}$$

$$C = \begin{bmatrix} 0 & 0 & 0 & 0 & 1 \end{bmatrix}$$

$$D = \begin{bmatrix} 0 \end{bmatrix}$$

(1.19)

Small signal transfer function from above equation by takin Laplace transform.

$$\frac{w}{d} = C[sI - A^{-1}]B \qquad (1.20)$$

The transfer function of speed of the vehicle to input of duty cycle can be take out.

$$\frac{w}{d} = \frac{-s^2 - 800s + 480}{s^5 + 800s^4 + 2000s^3 + 7100s^2 + 1600s + 110}$$

(1.21)

This transfer function is the fifth order function which can be reduced into second order transfer function. The reduced transfer function is as follows:

$$\frac{w}{d} = \frac{-s + 800}{s^2 + 143s + 320} \qquad (1.22)$$

The bode plot of a plant and the reduced transfer function of the system can be in fig.5

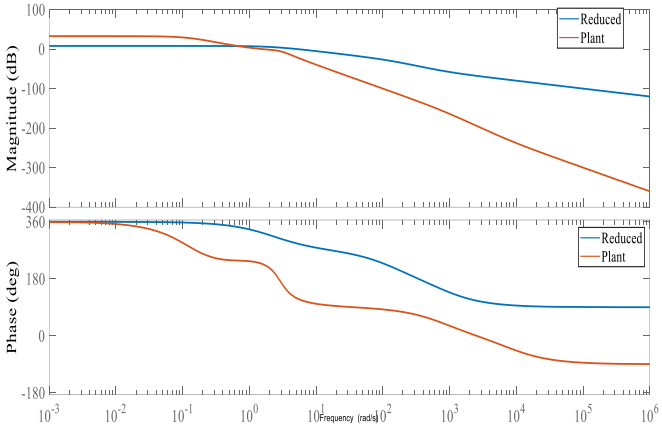

Figure 5: Bod plot of the plant and reduced order.

International Journal of Engineering Research & Technology (IJERT)
ISSN: 2278-0181
Vol. 11 Issue 11, November-2022

4.CONTROLLER DESIGN

4.1 Adaptive Controller

Adaptive control is a method of designing a controller with some adjustable parameters and an embedded mechanism for adjusting these parameters. From different adaptive control approach in this paper model reference adaptive control is selected. The model reference adaptive system is a method of comparing the performance of the actual system against an assumed mathematical model that describes the actual system, and designing control input to drive this comparison error to zero [5,12].

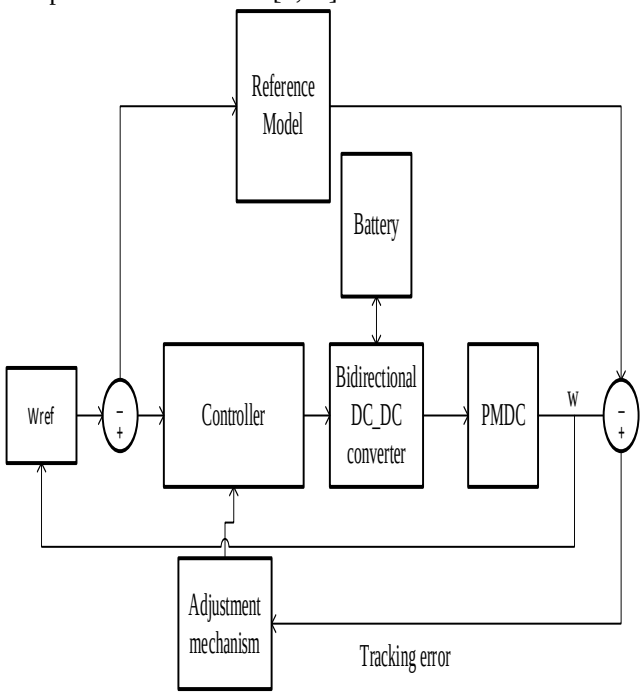

Figure 6. Block diagram of proposed model with controller

4.2 Model Reference Adaptive PI Control

In this thesis, PI can't control the overall system because the system is highly nonlinear. Which means the coefficients of the conventional PI controller are not often property tuned for the nonlinear plant with unpredictable parameter variations. To improve the problem of this model reference adaptive controller is used in order to adjust PI parameters.
The plant transfer function is given by:

$$\frac{w(s)}{u(s)} = \frac{-s+a}{s^2+b_1 s+b_2} \qquad (1.23)$$

Where a, b_1 and b_2 assume to be constant. Consider also the following PI control law), where the Laplace transform of the control signal is given by:

$$U(s) = K_p(U_c(s)-Y(s)) + \frac{K_i}{s}(U_c(s)-Y(s)) \qquad (1.24)$$

An important problem is to determine the adjustment mechanism so that a stable system that brings the error to zero, is obtained. The following parameter adjustment mechanism, called the MIT rule was originally used in MRAC:

$$\frac{d\theta}{dt} = -\gamma e \frac{\partial e}{\partial \theta} \qquad (1.25)$$

e ($e = y - y_m$) denotes the model error. The components of $\frac{\partial e}{\partial \theta}$ are the sensitivity derivatives of the error with respect to the adjustable parameter vector θ .The parameter γ is known as the adaptation gain. The adjustment mechanism is to minimize the squared model error e^2 . The cost function is:

$$J(\theta) = \frac{1}{2}e^2(\theta) \qquad (1.26)$$

The closed loop transfer function of the plant can be:

$$Y(s) = \frac{-k_p s^2 + s(k_p a - k_i) + k_i a}{s^3 + s^2(b_1 - k_p) + s(b_2 - k_i + k_p a) + k_i a} U_c(s) \qquad (1.27)$$

According to the closed form transfer function in (1.26), we select a second order system as the reference model:

$$\frac{Y_m}{U_m} = \frac{900}{s^2+30s+900} \qquad (1.28)$$

If Y= Y_m, the input –output relations of the system and the model are the same, this is called perfect modeling. The model error is defined as the difference between the process output Y and the reference model output Y_m ($e = Y - Y_m$). It is then possible to derive adaptation rules for the controller parameter vector $\theta = (k_p, k_i)$ of control law (1.25) using MIT rule:

$$\frac{d\theta}{dt} = -\gamma e \frac{\partial e}{\partial \theta} \qquad (1.29)$$

$$\frac{dK_p}{dt} = -\gamma \frac{\partial J}{\partial K_p} = -\gamma \frac{\partial J}{\partial e}\frac{\partial e}{\partial Y}\frac{\partial Y}{\partial K_p}$$

$$\frac{dK_i}{dt} = -\gamma \frac{\partial J}{\partial K_i} = -\gamma \frac{\partial J}{\partial e}\frac{\partial e}{\partial Y}\frac{\partial Y}{\partial K_i} \qquad (1.30)$$

Where $\frac{\partial J}{\partial e} = e, \frac{\partial e}{\partial Y} = 1$

we get following equations:

$$k^*_p = \frac{-\gamma_p}{s} e\left(\frac{-s^2+sa}{s^3+s^2(b_1-k_p)+s(b_2-k_i+k_p a)+k_i a}\right)(u_c - y) \qquad (1.31)$$

$$k_i^* = \frac{-\gamma_i}{s} e\left(\frac{-s^2+a}{s^3+s^2(b_1-k_p)+s(b_2-k_i+k_p a)+k_i a}\right)(u_c - y) \qquad (1.32)$$

Where(b_1-K_p), (b_2-k_i+k_pa) and (k_ia) are variables which can be determined from reference model.

5. SIMULATION RESULTS AND DISCUSSION

International Journal of Engineering Research & Technology (IJERT)
ISSN: 2278-0181
Vol. 11 Issue 11, November-2022

To verify the validity of the proposed method, the simulation has been performed. Simulation parameters was selected from previously done journals [12]. A total of two cases of the drive system are studied: cas1: The reference motor speed is 52 rad/sec with a constant torque demand of 6Nm, when the speed changes from 52 rad/sec(500rpm) to 62 rad/sec with a constant torque demand of 10 Nm at time t=15 secs and case (2) regenerative braking mode: when the speed decreases. Torque changes from +10 Nm to -10 Nm at a step time of 15 secs. The simulation is carried out.

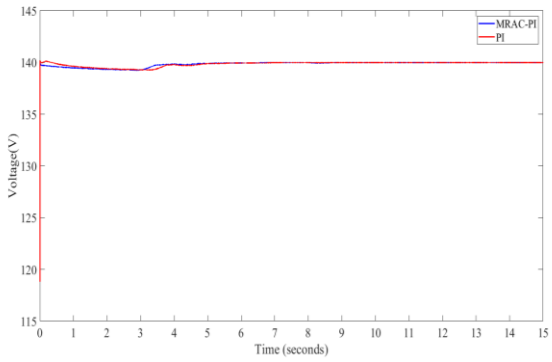

Figure7. Battery voltage.

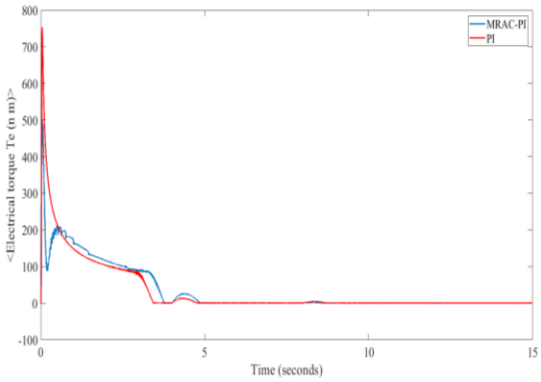

Figure 8. Electrical torque

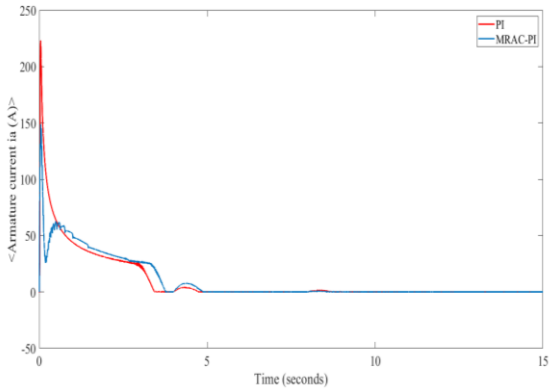

Figure 7 and 8 show battery voltage and motor torque respectively during forward and breaking mode of conversion. During transient, simulations are performed when the motor speed is changed from 52 rad/sec to 62rad/sec. Momentarily increase in torque when there is a

Figure 9. Motor current.

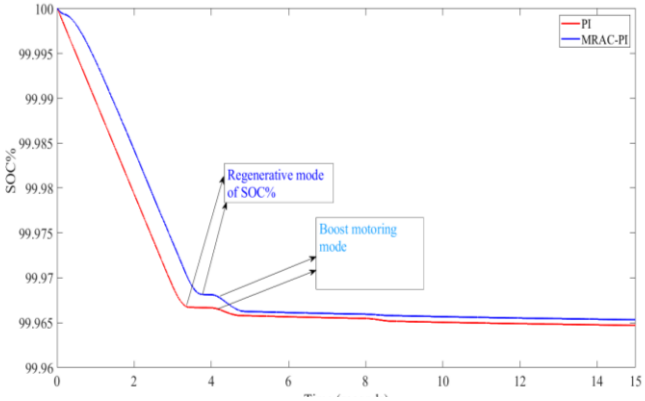

Figure 10. Battery State of charge.

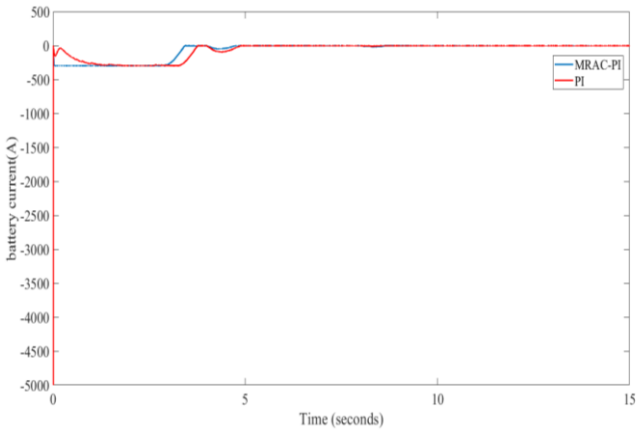

Figure 11. Battery Current

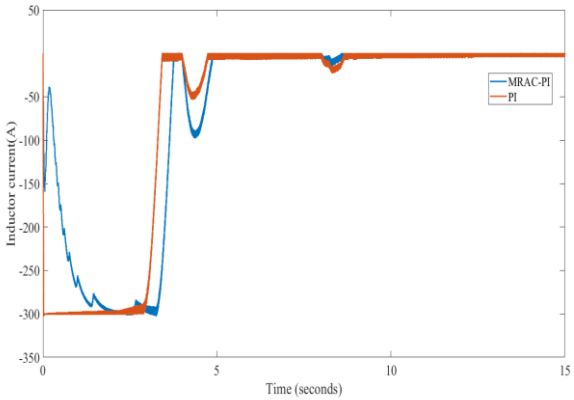

Figure 12. Inductor current

sudden change in speed requirement. The motor current which is same as the torque characteristic. When the speed increases, the motor draws more power from the battery as, the battery SOC discharging and buck mode condition. When the speed decreases, the battery SOC charging and boost mode condition in figure 10. The Simulations are also performed for the braking operation when the speed is changed from 52 rad/sec to 50 rad/sec while the motor

International Journal of Engineering Research & Technology (IJERT)
ISSN: 2278-0181
Vol. 11 Issue 11, November-2022

torque and current has reverse characteristic as shown in Figure 8 and Figure 9 respectively between 3sec to 4 secs. Figure 11 and 12 show the battery current and inductor current under this condition.

CONCLUSION

In this work we demonstrate the performance of a bidirectional DC-DC converter for electric vehicle system and its performance at different driving condition. The proposed control technique with MRAC_PI controller find suitable for this electric drive. The performance of the system is verified under forward motoring mode, regenerative mode. The converter mode is determined not only by the relationship between the voltage on the DC-bus and its set voltage value of 140 V, but also by the relationship between the DC-bus voltage and the energy storage battery. To optimize the system, the controller would have to be able to switch from Buck mode to Boost mode by use the derivative of the inductor current to determine the converter mode. If the converter is in Buck mode and the current slope is to low or decreasing, the converter could change to Boost mode and therefore draw a higher current. This would improve the converters overall performance and efficiency.

REFERENCES

[1] G. Y. Choe, J. S. Kim, B. K. Lee, C. Y. Won, T. W. Lee," A bi-directional battery charger for electric vehicles using photovoltaic PCS systems", Proc. IEEE Veh. Power Propulsion Conf., pp. 1-6, 2010.

[2] R. T. Naayagi, A. J. Forsyth, and R. Shuttleworth, "Bidirectional control of a dual bridge DC-DC converter for aerospace applications," Power Electronics, IET, vol. 5, pp.1104-1118, 2012.

[3] K. Minho, O. Secheol, and C. Sewan, "High Gain Soft-Switching Bidirectional DCDC Converter for Eco-Friendly Vehicles," Power Electronics, IEEE Transactions on, vol. 29,pp. 1659-1666, 2014

[4] P. Junsung and C. Sewan, "Design and Control of a Bidirectional Resonant DC-DC Converter for Automotive Engine/Battery Hybrid Power Generators," Power Electronics, IEEE Transactions on, vol. 29, pp. 3748-3757, 2015.

[5] K. Engelen, S. De Breucker, P. Tant, and J. Driesen, "Gain scheduling control of a bidirectional dc-dc converter with large dead-time," Power Electronics, IET, vol. 7, pp.480-488, 2014.

[6] R. Guzman, L. J. Garcia de Vicuna, J. Morales, M. Castilla, and J. Matas, "SlidingMode Control for a Three-Phase Unity Power Factor Rectifier Operating at Fixed Switching Frequency," Power Electronics, IEEE Transactions on, vol. PP, pp. 1-1, 2015.

[7] I. Gowaid, G. Adam, A. Massoud, S. Ahmed, D. Holliday, B. Williams. "Quasi TwoLevel Operation of Modular Multilevel Converter for Use in a High-Power DC Transformer with DC Fault Isolation Capability". IEEE Transactions on Power Electronics, vol. 30, No. 1, Jan 2016.

[8] P. Giannelli, M. Rossi, L. Capineri, M. Granato, G. Frattini, and G.Calabrese, "The ZetaBoost: A step-up DC/DC topology derived from the zeta converter," in 2017 18th European Conference on Power Electronics and Applications, 2017, pp. 1–10

[9] Y. Wang, L. Xue, C. Wang, P. Wang, W, Lei. "Interleaved High-Conversion-Ratio Bidirectional DC–DC Converter for Distributed Energy-Storage Systems—Circuit Generation, Analysis, and Design".IEEE Transactions on Power Electronics. vol. 31, No. 18. Aug 2018.

[10] Rehman M M U, Zhang F, Zane R, et al. Control of bidirectional DC/DC converters in reconfigurable, modular battery systems. Applied Power Electronics Conference and Exposition (APEC), 2019 IEEE. IEEE, 2019: 1277-1283.

[11] Greg Stahl, Miguel Rodriguez, and DraganMaksimovic,"A High-Efficiency Bidirectional Buck-Boost DC-DC Converter," IEEE AppliedPower Electronics Conference and Exposition (APEC)., 1362-1367, Feb. 2020.

[12] Seung-Ryul Moon, Ki-Chang Lee, Jong-Moo Kim, Dae-Hyun Koo,"Closed-Loop Regenerative Efficiency Testing with Electric Vehicle Bidirectional Dc-dc Converter," IEEE Applied Power ElectronicsConference and Exposition (APEC)., 2461-2466, Feb. 2021.